JPE 13-3-10

http://dx.doi.org/10.6113/JPE.2013.13.3.419

Multivariable Optimal Control of a Direct AC/AC Converter under Rotating *dq* Frames

Yun Wan[†**], Steven Liu[**], and Jianguo Jiang[*]

[†*]Key Laboratory of Control of Power Transmission and Conversion, Ministry of Education
Shanghai Jiao Tong University, Shanghai, China
[**]Institute of Control Systems, University Kaiserslautern, Kaiserslautern, Germany

Abstract

The modular multilevel cascade converter (MMCC) is a new family of multilevel power converters with modular realization and a cascaded pattern for submodules. The MMCC family can be classified by basic configurations and submodule types. One member of this family, the Hexverter, is configured as Double-Delta Full-Bridge (DDFB). It is a novel multilevel AC/AC converter with direct power conversion and comparatively fewer required components. It is appropriate for connecting two three-phase systems with different frequencies and driving an AC motor directly from a utility grid. This paper presents the *dq* model of a Hexverter with both of its AC systems by state-space representation, which then simplifies the continuous time-varying model into a periodic discrete time-invariant one. Then a generalized multivariable optimal control strategy for regulating the Hexverter's independent currents is developed. The resulting control structure can be adapted to other MMCCs and is flexible enough to include other control criterion while guaranteeing the original controller performance. The modeling method and control design are verified by simulation results.

Key words: *dq* modeling, Hexverter, Modular multilevel cascade converter (MMCC), Multivariable optimal control

I. INTRODUCTION

Nowadays, the modular multilevel converter family, which is also called the modular multilevel cascade converter (MMCC) family, has aroused a great of attention in terms of scientific research and industrial applications [1]-[3]. This began when Marquardt, R. presented and validated the Modular Multilevel Converter (MMC) topology under laboratory conditions [4] and Siemens implemented the HVDC-Plus project with two back-to-back (BTB) configured MMCs in industrial practice [5]. By comparing with an indirect AC/AC conversion based on BTB-MMCs, Baruschka, L. and Mertens, A. proposed a new three-phase direct AC/AC modular multilevel converter with six branches in a hexagonal configuration, which is called a Hexverter [6], [7]. The Hexverter realizes a direct AC/AC conversion between two three-phase systems and requires a smaller number of submodules (SM) than BTB-MMCs and modular multilevel matrix converters (M3C) [6], [8]. Therefore, a Hexverter can be applied to connect two grids with different frequencies and drive a three-phase motor from a utility grid.

In [6] and [7], the authors described the Hexverter topology, developed its state-space modeling in the *αβ* frame, analyzed the operational principal and verified it with an experimental prototype. However, the derivation of the Hexverter *dq* model and the design of a complete control strategy remain open questions. First a state-space model of a Hexverter in the *dq* frames will be developed in this paper in order to utilize the advantages of controlling power converters in the synchronous rotating frame. Thanks to the *dq* transformation, the fundamental components of the current variables are transformed into DC components, which can simplify the controller design and improve the performance at the fundamental frequency.

Manuscript received Jan. 19, 2013; revised Mar. 4, 2013
Recommended for publication by Associate Editor Se-Kyo Chung.
[†]Corresponding Author: wan@eit.uni-kl.de
Tel: +49-(0)631-205-3656, Fax: +49-(0)631-205-4205, Shanghai Jiao Tong Univ.
[*]Key Laboratory of Control of Power Transmission and Conversion, Ministry of Education Shanghai Jiao Tong University, China
[**]Institute of Control Systems, University Kaiserslautern, Kaiserslautern, Germany

Another important issue for the Hexverter as well as the other topologies in the MMCC family is their large quantity of control requirements, such as multiple independent current tracking, numerous switching combinations and internal branch energy balancing. This increases the difficulty of designing the commonly used parallel or cascaded multi-PI(D)s control structures while dealing with complicated coupling, laborious PI parameters determination, a unpredictable closed-loop convergence rate and full utilization of the high-degree freedom [9]. Furthermore, the control design is far from an integrated and unified method for fulfilling all of the control requirements. A state feedback control for multivariable systems shows its advantages in handling the aforementioned problems. In [10] and [11], a complete multivariable design is developed to control the current variables, compensate the harmonics and balance the internal energy distribution for the MMC. The idea for this control design can be described briefly as: a linear multivariable model for the investigated system is required and a quadratic cost function **J** is defined based on the concerning control criterion. A control law, which is also the state feedback gain **K**, can be determined by minimizing the cost function **J**. This design method, called a linear quadratic regulator (LQR), guarantees a compromise between the control efforts and the response speed, which inherently achieves a stable system. Furthermore, it is a generalized method and can be easily applied to other MMCC systems.

This paper presents the *dq* modeling of the Hexverter with both-side AC systems connected and an optimal multivariable control design. First a brief classification of the MMCC is provided and the topology of the Hexverter is introduced. Then the Hexverter modeling in the *abc* frame, the double-SDFB equivalent method and the derivation of its *dq* state-space model are successively presented. In the following section, a generalized multivariable control design intended for regulating multiple current variables and rejecting the grid-side disturbances is analyzed. Finally the system operations and controller performance are verified by simulation results.

II. CLASSIFICATION OF MMCCS AND THE DOUBLE-DELTA FULL-BRIDGE MMCC – HEXVERTER

As described in [2],[3], the modular multilevel cascade converter (MMCC) is a family of emerging multilevel converters which are configured with the cascaded connection of full-bridge (FB) or half-bridge (HB) submodules by distinct topological structures. All of the existing MMCC topologies can be classified by their three-phase connection types as either star- or delta-connection-based MMCCs [2], [3]. A detailed classification is given in Table I.

TABLE I
CLASSIFICATION OF MMCC FAMILY

	Configuration	SM type
Star-connection -based MMCCs	Single-Star Full-Bridge (SSFB) [2]	FB
	Double-Star Half-Bridge (MMC) [12]	HB
	Double-Star Full-Bridge (DSFB) [13]	FB
	Double-Star Half-Bridge Back-to-Back (Indirect MMC) [14]	HB
	Triple-Star Full-Bridge (Modular Multilevel Matrix Converter, M3C, "Chainlink" converter) [15]	FB
Delta-connection -based MMCCs	Single-Delta Full-Bridge (SDFB) [2],[16]	FB
	Double-Delta Full-Bridge (DDFB, Hexverter) [6],[7]	FB

This paper discusses the Double-Delta Full-Bridge MMCC (Hexverter). The Hexverter is constituted by six branches, each of which contains a branch inductor and a certain number of cascaded FB submodules. The DDFB-MMCC is called the Hexverter, because the ring-type connection of the converter's six identical branches can be regarded as a hexagon. The combination of the words "hexagon" and "converter" produce the name "hex-verter". The following discussion will be based on the obtained model in the *abc* frame and extended to the *dq* frames by converting the Hexverter into two Single-Delta Full-Bridge structures. A multivariable optimal control strategy will be accordingly proposed based on the state-space representation.

III. STATE SPACE MODEL OF THE HEXVERTER UNDER THE ROTATING *dq* FRAMES

A. Hexverter Modeling

The Hexverter is configured by six FB-submodule branches into a hexagonal shape and it contains six terminals that connect to two different three-phase AC systems (System1-UVW and System2-RST), as shown in Fig.1(a). u_U , u_V and u_W are the terminal voltages from System1-UVW and u_R , u_S and u_T are the terminal voltages from System2-RST. The six terminal currents are also plotted with the definition of their positive directions. Take one branch between terminal S and W, signed as Branch-SW. R and L are the resistance and inductance from the branch inductor of Branch-SW. The controllable branch voltage u_{SW} originates from the cascaded FB-SMs and the branch current i_{SW} flows continuously through Branch-SW. Note that the six branches in the Hexverter carry continuous branch currents during run time, and a continuous mathematical modeling can be expected when compared with the conventional two-level converter with switched system

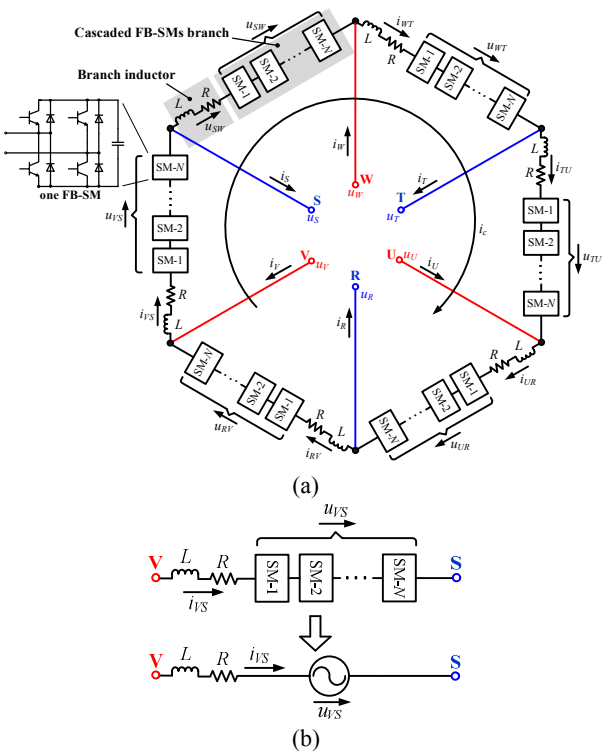

Fig. 1. Schematic diagram and branch equivalent circuit of Hexverter.

modeling. The cascaded FB-SMs branch can be equivalent to a controllable voltage source, as illustrated in Fig.1(b) with Branch-VS as an example. The Hexverter's AC-side systems (resistors, inductors and voltage sources or electromotive forces) are introduced later and a complete modeling for the Hexverter with its connected two AC systems under the rotating *dq* frames will be given at the end of this section.

Another important definition in Fig.1(a) is the unique circular current i_c flowing in the hexagonal structure. According to the definition of the circulating current in MMCCs, it is a current that has no emergence at any of the MMCC terminals and flows only through its branches [3]. Therefore, there exists one and only one circulating current in the Hexverter, which is given as:

$$i_c = \frac{1}{6}(i_{UR} + i_{RV} + i_{VS} + i_{SW} + i_{WT} + i_{TU})$$

By adjusting the six branch voltages, the circulating current can be adjusted to cope with the following two situations:

(1) In dynamic operation, the circulating current can be controlled in order to achieve a preferred energy adjustment and distribution among branches;

(2) In steady state operation, the circulating current can be eliminated or suppressed to its minimum, while its DC component increases the branch energy difference and its AC components cause unnecessary additional branch energy fluctuations.

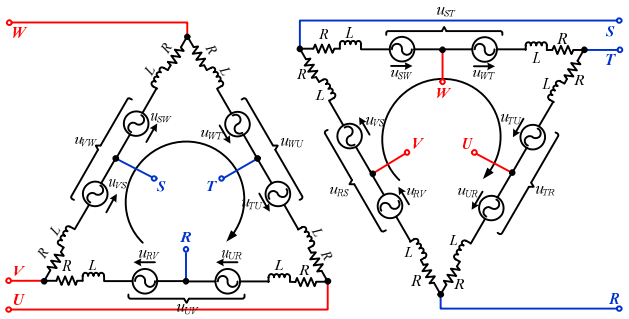

Fig. 2. The reconfigured "Single-Delta"-based Hexverter.

By selecting the four terminal currents i_U, i_V, i_R, i_S and the only circulating current i_c as state variables $\mathbf{x}$, the rest of the current variables in the Hexverter can be completely expressed. The six branch voltages act as control inputs $\mathbf{u}$ and the terminal voltages act as disturbances $\mathbf{v}$. The state-space equations (SSEs) for the Hexverter can be given as:

$$\dot{\mathbf{x}} = \mathbf{A}\mathbf{x} + \mathbf{B}\mathbf{u} + \mathbf{E}\mathbf{v} \tag{1}$$

where $\mathbf{x} = [i_U \quad i_V \quad i_R \quad i_S \quad i_c]^T$

$\mathbf{u} = [u_{UR} \quad u_{RV} \quad u_{VS} \quad u_{SW} \quad u_{WT} \quad u_{TU}]^T$

$\mathbf{v} = [u_U \quad u_V \quad u_W \quad u_R \quad u_S \quad u_T]^T$

$\mathbf{A} = \mathrm{diag}\left(-\frac{R}{L}, -\frac{R}{L}, -\frac{R}{L}, -\frac{R}{L}, -\frac{R}{L}, -\frac{R}{L}\right)$

$$\mathbf{B} = \begin{bmatrix} -1/L & 0 & 0 & 0 & 0 & 1/L \\ 0 & 1/L & -1/L & 0 & 0 & 0 \\ -1/L & 1/L & 0 & 0 & 0 & 0 \\ 0 & 0 & -1/L & 1/L & 0 & 0 \\ -\frac{1}{6L} & -\frac{1}{6L} & -\frac{1}{6L} & -\frac{1}{6L} & -\frac{1}{6L} & -\frac{1}{6L} \end{bmatrix}$$

$$\mathbf{E} = \begin{bmatrix} 2/L & 0 & 0 & -1/L & 0 & -1/L \\ 0 & 2/L & 0 & -1/L & -1/L & 0 \\ 1/L & 1/L & 0 & -2/L & 0 & 0 \\ 0 & 1/L & 1/L & 0 & -2/L & 0 \\ 0 & 0 & 0 & 0 & 0 & 0 \end{bmatrix}$$

B. The Equivalent Method for Analyzing the Hexverter

Each branch in the Hexverter connects two terminals with different fundamental frequencies, which indicates that each branch voltage in $\mathbf{u}$ contains voltage components from both frequencies. Consequently, an immediate application of the Park transformation to (1) encounters difficulty in dealing with the control inputs $\mathbf{u}$ dominated by multiple frequencies.

In order to derive the *dq* model of the Hexverter, it is necessary to introduce the concept that the double-delta-configured Hexverter can be considered as two independent SDFB-MMCCs with their respective frequencies, as shown in Fig.2. Suppose System1-UVW has an angular velocity ω_1 and System2-RST has an angular velocity ω_2.

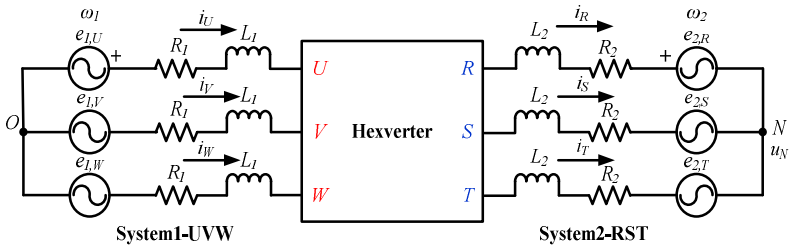

Fig. 3. Model of Hexverter with both-side AC systems.

The six new variables labeled in Fig.2 can then be defined as:

$$\begin{cases} u_{UV} = u_{UR} + u_{RV} \\ u_{VW} = u_{VS} + u_{SW} \\ u_{WU} = u_{WT} + u_{TU} \\ u_{TR} = u_{TU} + u_{UR} \\ u_{RS} = u_{RV} + u_{VS} \\ u_{ST} = u_{SW} + u_{WT} \end{cases} \tag{2}$$

The newly defined branch voltage u_{UV}, which is the sum of the two branch voltages u_{RV} and u_{UR}, contains only the AC component with the frequency ω_1, while the branch voltage u_{TR} contains only the frequency component of ω_2. The other four variables u_{VW}, u_{WU}, u_{RS} and u_{ST} are constituted by the single frequency component and their frequencies are decided by the frequencies of their attached AC systems. Note that only the four equations in (2) are independent and two new variables are still needed to fully substitute for the original six branch voltages.

An independent variable, called the loop voltage $u_{b\Sigma}$, can be defined as the sum of all six branch voltages

$$u_{b\Sigma} = u_{UR} + u_{RV} + u_{VS} + u_{SW} + u_{WT} + u_{TU} \tag{3}$$

This can be used to adjust the circulating current i_c. The last expression relates the potential difference between the neutral points from System1 and System2, which will be derived in the following analysis of the Hexverter AC-side connections.

C. Hexverter with Both -Side AC Systems

The both AC-side connections of the Hexverter are depicted, as shown in Fig.3. The two systems adopt star connections with their neutral points O and N. The three-phase voltage sources from System1-UVW and System2-RST can be written as:

$$\begin{cases} e_{1,U} = E_1 \cos(\varphi_1) \\ e_{1,V} = E_1 \cos(\varphi_1 - \frac{2\pi}{3}) \\ e_{1,W} = E_1 \cos(\varphi_1 + \frac{2\pi}{3}) \end{cases} \text{and} \quad \begin{cases} e_{2,R} = E_2 \cos(\varphi_2) \\ e_{2,S} = E_2 \cos(\varphi_2 - \frac{2\pi}{3}) \\ e_{2,T} = E_2 \cos(\varphi_2 + \frac{2\pi}{3}) \end{cases}$$

where $\varphi_1 = \theta_1 + \omega_1 t$, $\varphi_2 = \theta_2 + \omega_2 t$, and θ_1 and θ_2 are the initial phase angles for System1 and System2, respectively. In this paper, it is assumed that the magnitudes and phase angles can be fully obtained by voltage transformers and PLLs.

The voltage between N and O is called u_N and it can be expressed by the six branch voltages as:

$$u_N = \frac{1}{6}(u_{UR} - u_{RV} + u_{VS} - u_{SW} + u_{WT} - u_{TU}) \tag{4}$$

Note that the floating voltage u_N can be used together with i_c to adjust the branch power in dynamics [6].

With (3), (4) and the four independent equations in (2), a complete transformation from the control inputs with double-frequencies to new ones with single-frequencies can be achieved as:

$$\begin{bmatrix} u_{UV} \\ u_{VW} \\ u_{TR} \\ u_{RS} \\ u_N \\ u_{b\Sigma} \end{bmatrix} = \begin{bmatrix} 1 & 1 & 0 & 0 & 0 & 0 \\ 0 & 0 & 1 & 1 & 0 & 0 \\ 1 & 0 & 0 & 0 & 0 & 1 \\ 0 & 1 & 1 & 0 & 0 & 0 \\ 1/6 & -1/6 & 1/6 & -1/6 & 1/6 & -1/6 \\ 1 & 1 & 1 & 1 & 1 & 1 \end{bmatrix} \begin{bmatrix} u_{UR} \\ u_{RV} \\ u_{VS} \\ u_{SW} \\ u_{WT} \\ u_{TU} \end{bmatrix}$$

$$\mathbf{u}_{new} = \mathbf{T}_u \mathbf{u} \quad \text{or} \quad \mathbf{u} = \mathbf{T}_u^{-1} \mathbf{u}_{new} \tag{5}$$

Another necessary adaption for (1) is to rewrite the disturbance $\mathbf{v}$ when two AC systems are connected:

$$\mathbf{v} = \mathbf{v}_{new} + \mathbf{u}_N - \mathbf{R}_{AC}\mathbf{x} - \mathbf{L}_{AC}\dot{\mathbf{x}} \tag{6}$$

where $\mathbf{v}_{new} = \begin{bmatrix} u_{1,U} & u_{1,V} & u_{1,W} & u_{2,R} & u_{2,S} & u_{2,T} \end{bmatrix}^T$, $\mathbf{u}_N = \begin{bmatrix} 0 & 0 & 0 & u_N & u_N & u_N \end{bmatrix}^T$, and $\mathbf{R}_{AC}$ and $\mathbf{L}_{AC}$ are the parameter matrices with regards to the both AC-side resistance and inductance, respectively. Substituting (5) and (6) back into (1) gives:

$$\dot{\mathbf{x}} = \mathbf{A}'\mathbf{x} + \mathbf{B}'\mathbf{u}_{new} + \mathbf{E}'\mathbf{v}_{new} \tag{7}$$

After the above pretreatment to the state-space equations (1), the *dq* model of the Hexverter can then be obtained.

D. Model of Hexverter under the dq Frames Connecting Two AC systems

By applying accordingly the Clark and Park transformation matrices to the state variables $\mathbf{x}$, control inputs $\mathbf{u}_{new}$ and disturbances $\mathbf{v}_{new}$, the *dq* variables can be obtained by:

$$\mathbf{x} = \mathbf{T}_{2s/3s,x}\mathbf{T}_{2r/2s,x}\mathbf{x}_{dq}$$

$$\mathbf{u}_{new} = \mathbf{T}_{\mathbf{2s/3s,u}}\mathbf{T}_{\mathbf{2r/2s,u}}\mathbf{u}_{\mathbf{dq}}$$

$$\mathbf{v}_{new} = \mathbf{T}_{\mathbf{2s/3s,v}}\mathbf{T}_{\mathbf{2r/2s,v}}\mathbf{v}_{\mathbf{dq}}$$

where $\mathbf{x}_{\mathbf{dq}} = \begin{bmatrix} i_{UVW,d} & i_{UVW,q} & i_{RST,d} & i_{RST,q} & i_c \end{bmatrix}^T$, $\mathbf{u}_{\mathbf{dq}} = \begin{bmatrix} u_{UVW,d} & u_{UVW,q} & u_{RST,d} & u_{RST,q} & u_N & u_{b\Sigma} \end{bmatrix}^T$, $\mathbf{v}_{\mathbf{dq}} = \begin{bmatrix} e_{1,d} & e_{1,q} & e_{1,0} & e_{2,d} & e_{2,q} & e_{2,0} \end{bmatrix}^T$, and $\mathbf{T}_{\mathbf{2s/3s,x}}$, $\mathbf{T}_{\mathbf{2s/3s,u}}$ and $\mathbf{T}_{\mathbf{2s/3s,v}}$ are the Clark transformation matrices for the state variables, control inputs $\mathbf{u}$ and disturbances. $\mathbf{T}_{\mathbf{2r/2s,x}}$, $\mathbf{T}_{\mathbf{2r/2s,u}}$ and $\mathbf{T}_{\mathbf{2r/2s,v}}$ are the corresponding Park transformation matrices which transform the composite frequency components in the stationary *abc* frame to DC components in the two *dq* frames due to the both-side AC systems at different frequencies. All the transformation matrices can be found in the Appendix. Furthermore, by adopting the approximation where the branch inductance L and branch resistance are much smaller than the AC-side inductances L_1 and L_2, a simplified *dq* model of the Hexverter can finally be given as:

$$\dot{\mathbf{x}}_{\mathbf{dq}} = \mathbf{A}_{\mathbf{dq}}\mathbf{x}_{\mathbf{dq}} + \mathbf{B}_{\mathbf{dq}}(t)\mathbf{u}_{\mathbf{dq}} + \mathbf{E}_{\mathbf{dq}}\mathbf{v}_{\mathbf{dq}} \tag{8}$$

where

$$\mathbf{A}_{\mathbf{dq}} = \begin{bmatrix} -\frac{R_1}{L_1} & \omega_1 & 0 & 0 & 0 \\ -\omega_1 & -\frac{R_1}{L_1} & 0 & 0 & 0 \\ 0 & 0 & -\frac{R_2}{L_2} & \omega_2 & 0 \\ 0 & 0 & -\omega_2 & -\frac{R_2}{L_2} & 0 \\ 0 & 0 & 0 & 0 & -\frac{R}{L} \end{bmatrix}$$

$$\mathbf{B}_{\mathbf{dq}}(t) = \begin{bmatrix} -\frac{1}{2L_1} & -\frac{\sqrt{3}}{6L_1} & 0 & 0 & -\frac{8\sqrt{3}}{3L_1}\sin(\varphi_1+\frac{\pi}{3}) & \frac{2\sqrt{3}}{9L_1}\sin(\varphi_1+\frac{\pi}{3}) \\ \frac{\sqrt{3}}{6L_1} & -\frac{1}{2L_1} & 0 & 0 & \frac{8\sqrt{3}}{3L_1}\sin(\varphi_1-\frac{\pi}{6}) & -\frac{2\sqrt{3}}{9L_1}\sin(\varphi_1-\frac{\pi}{6}) \\ 0 & 0 & -\frac{1}{2L_2} & \frac{\sqrt{3}}{6L_2} & -\frac{8\sqrt{3}}{3L_2}\sin\varphi_2 & \frac{2\sqrt{3}}{9L_2}\sin\varphi_2 \\ 0 & 0 & -\frac{\sqrt{3}}{6L_2} & -\frac{1}{2L_2} & -\frac{8\sqrt{3}}{3L_2}\cos\varphi_2 & \frac{2\sqrt{3}}{9L_2}\cos\varphi_2 \\ 0 & 0 & 0 & 0 & 0 & -\frac{1}{6L} \end{bmatrix}$$

$$\mathbf{E}_{\mathbf{dq}} = \begin{bmatrix} \frac{1}{L_1} & 0 & \frac{2\sqrt{6}}{3L_1}\sin(\varphi_1+\frac{\pi}{3}) & 0 & 0 & -\frac{2\sqrt{6}}{3L_1}\sin(\varphi_1+\frac{\pi}{3}) \\ 0 & \frac{1}{L_1} & \frac{2\sqrt{6}}{3L_1}\cos(\varphi_1+\frac{\pi}{3}) & 0 & 0 & \frac{2\sqrt{6}}{3L_1}\cos(\varphi_1+\frac{\pi}{3}) \\ 0 & 0 & \frac{2\sqrt{6}}{3L_2}\sin\varphi_2 & -\frac{1}{L_2} & 0 & -\frac{2\sqrt{6}}{3L_2}\sin\varphi_2 \\ 0 & 0 & \frac{2\sqrt{6}}{3L_2}\cos\varphi_2 & 0 & -\frac{1}{L_2} & -\frac{2\sqrt{6}}{3L_2}\cos\varphi_2 \\ 0 & 0 & 0 & 0 & 0 & 0 \end{bmatrix}$$

Note that the fully measurable disturbance term $\mathbf{E}_{\mathbf{dq}}\mathbf{v}_{\mathbf{dq}}$ can be considered in the feedforward control. Therefore, it can be neglected in the following state feedback control design. The final system model (8) can be written into a general form as (For simplicity in writing and generality in illustration, the subscripts *dq* are removed in the following derivations.):

$$\dot{\mathbf{x}} = \mathbf{A}\mathbf{x} + \mathbf{B}(t)\mathbf{u} \tag{9}$$

By inspecting the index matrices in (9), it can be seen that the system equations reveal a multivariable (multi-input, multi-output, or MIMO) feature, complicated coupling effects and time-varying characteristics, which will increase the difficulty of designing the traditional multiple-PI(D)-based control structure. Furthermore, the cascaded or paralleled multi-PI(D) configuration results in a unpredictable longer oscillation until the steady state and inexplicit parameter determination. Therefore, a multi-variable control (MVC) design will be proposed to handle the coupling and multivariable. It should be mentioned that the difference voltage u_N is set to zero and removed from $\mathbf{u}$ in the following control design, so that a square and invertible control matrix $\mathbf{B}_s(t)$ can be obtained by removing the 5th column from $\mathbf{B}(t)$ in (9).

IV. Multivariable Optimal Control Design

In this section a LQR design for controlling the derived Hexverter's multivariable model is described. In order to apply the LQR method, the original linear time-varying (LTV) model (9) is modeled as a *p*-periodic LTV system with the so-called hyper-period, and further discretized into a periodic discrete system with the p linear time-invariant (LTI) subsystems in each hyper-period (p is an integral). As a result, the LTV model (9) can be simplified into a *p*-periodic discrete LTI system with a specific discretization period, which can be solved by the periodic discrete LQR (PDLQR) method. The method of periodic discrete modeling and the PDLQR design are unified and characterized by easy expansion to other MMCC topologies. For example, the unified method is investigated and verified for the MMC in [11],[17]. Note that the obtained periodic control gain from the PDLQR can only regulate the state variables to the origin while minimizing the chosen cost function. Therefore, a feedforward design to introduce the reference input will be required to control the state variables tracking their respective references. In the last section, the feedforward rejection of the measurable grid-side voltages is discussed to complete the whole control structure.

A. Periodic Modeling with the Hyper-Period

The index submatrix $\mathbf{B}_s(t)$ in the *dq* model of the Hexverter is time-varying and actually contains two periodic parameters, the phase angles φ_1 and φ_2 and their respective periods T_1 and T_2. To model it as a periodic system, its hyper-period T_h will be determined. First write

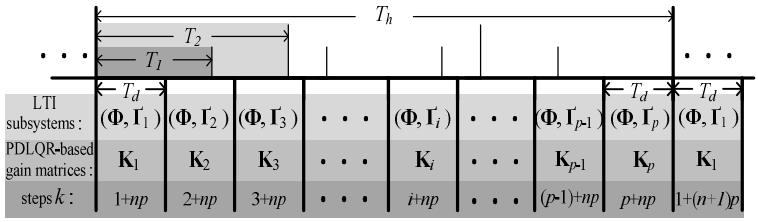

Fig. 4. Illustration of the periodic modeling, discretization and PDLQR.

T_1 and T_2 into the irreducible fraction formats as $\frac{a_1}{b_1}$ and $\frac{a_2}{b_2}$. The hyper-period T_h can be then calculated as:

$$T_h = \frac{\text{lcm}(a_1, a_2)}{\text{gcd}(b_1, b_2)}$$

where lcm(,) denotes the least common multiple of the two integers and gcd(,) calculates the greatest common divisor. For example, in the simulation example a Hexveter connects two three-phase grids with the respective periods of $\frac{1}{50}$ s (50Hz) and $\frac{1}{30}$ s (30 Hz). The hyper-period can be obtained as $\frac{1}{10}$ s, which also indicates that the period of the variables in $\mathbf{B}_s(t)$ is 0.1s.

B. Discretization of periodic LTV systems

After the hyper-period T_h is obtained, the *dq* model can be discretized by the discretization period T_d as:

$$T_d = T_h / p$$

where p is an integer number of samples per hyper-period. When the chosen value of p is large enough, the LTV system can be considered as LTI in each time interval T_d. In the later simulation, p is selected as 500, resulting a discretization time T_d of 0.2ms. A comprehensive presentation is summarized in the periodic control theory, which can be found in [18].

The system equation (9) can then be discretized by the selected discretization time T_d and modeled as a periodic discrete LTI system, which is satisfactory in each discretization period [19]:

$$\mathbf{x}(k+1) = \mathbf{\Phi}\mathbf{x}(k) + \mathbf{\Gamma}_i\mathbf{u}(k) \quad (10)$$

where $\mathbf{\Phi} = e^{\mathbf{A}T_d}$, $\mathbf{\Gamma}_i = \mathbf{A}^{-1}(\mathbf{\Phi} - \mathbf{I})\mathbf{B}_s((i-1)T_d)$, $k = i + n \cdot p$, $i \in \{1, 2, 3, ..., p\}$ and $n = 1, 2, 3, ...\infty$. The resultant discrete-time system (10) presents periodicity and time-invariant in each T_d, which can be regulated by a Periodic Discrete Linear Quadratic Regulator (PDLQR) with p-periodic control gains $\mathbf{K}_i$ ($i \in \{1, 2, .., p\}$) for each of the discretization periods.

C. PDLQR Design

The PDLQR method solves the periodic control gains for the periodic LTI subsystems with the classic LQR in each discretization period. The classic LQR theory for regulating a LTI system can be described as [18]: for a discrete-time LTI plant, a control law can be defined as the feedback of the multiplication of the control gain matrix $\mathbf{K}$ and the state variables $\mathbf{x}(k)$:

$$\mathbf{u}(k) = -\mathbf{K}\mathbf{x}(k) \quad (11)$$

such that the system can be regulated from its initial state $\mathbf{x}(0)$ to the origin while minimizing a predefined discrete-time quadratic cost function $\mathbf{J}$:

$$\mathbf{J} = \frac{1}{2}\sum_{k=0}^{\infty}[\mathbf{x}^T(k)\mathbf{Q}\mathbf{x}(k) + \mathbf{u}^T(k)\mathbf{R}\mathbf{u}(k)] \quad (12)$$

where $\mathbf{Q}$ indicates the symmetric nonnegative definite weighting matrices, namely the error weighted matrix, and $\mathbf{R}$ indicates the symmetric positive definite weighting matrices, namely the control weighted matrix, both of which are chosen by designers. The selections of $\mathbf{Q}$ and $\mathbf{R}$ indicate the relative importance of the state variables and control inputs, and they require a certain amount of trial and error to adjusting them to obtain a satisfactory control effect. The solution $\mathbf{K}$, corresponding to each pair of $\mathbf{Q}$ and $\mathbf{R}$, can be calculated by efficient computation tools. Because the solution is applied to a linear system, the cost function is in the quadratic form and it acts as a regulator. It is called linear quadratic regulator (LQR).

For the PDLQR design, in each time-invariant discretization interval, the discrete-time quadratic cost function $\mathbf{J}_{PD}$ can be accordingly given as:

$$\mathbf{J}_{PD} = \sum_{k=0}^{\infty}[\mathbf{x}^T(k)\mathbf{Q}_i\mathbf{x}(k) + \mathbf{u}^T(k)\mathbf{R}_i\mathbf{u}(k)] \quad (13)$$

where $\mathbf{Q}_i$ and $\mathbf{R}_i$ ($i = \text{mod}(k, p)$) are the i-th p-periodic error and the control weighted matrices in the k-th discretization interval, respectively. The solution method leads to the stationary algebraic Riccati equation (ARE) as:

$$\mathbf{P}_i = \mathbf{\Phi}^T(\mathbf{P}_i - \mathbf{P}_i\mathbf{\Gamma}_i(\mathbf{R}_i + \mathbf{\Gamma}_i^T\mathbf{P}_i\mathbf{\Gamma}_i)^{-1}\mathbf{\Gamma}_i^T\mathbf{P}_i)\mathbf{\Phi} + \mathbf{Q}_i \quad (14)$$

The solution for the above equation cannot always be analytic. However, it can be determined by efficient numerical methods. The computation methods can be found in [20],[21] and are implemented in Matlab. As a result, they are neglected in this paper. The positive-definite solution $\mathbf{P}_i$ for the algebraic matrix Riccati equation (14) can be obtained and it will result in a control law such that:

$$\mathbf{u}(k) = -[(\mathbf{R}_d + \mathbf{\Gamma}_i^T \mathbf{P}_i \mathbf{\Gamma}_i)^{-1} \mathbf{P}_i \mathbf{\Phi}]\mathbf{x}(k) = -\mathbf{K}_i \mathbf{x}(k) \quad (15)$$

where $\mathbf{K}_i$ is the *i*-th *p*-periodic time-invariant constant control gain matrix.

The aforementioned hyper-period determination, *p*-periodic discrete LTI model transformation and PDLQR -based control gain design are illustrated in Fig.4. To complete the whole control design, the methods for introducing a reference input [20] and for rejecting the measurable disturbances [22] are respectively proposed.

D. Introduction of the Reference Input

As mentioned previously, the designed PDLQR can simply regulate the periodic MIMO system from any initial states to the origin along the optimal trajectory defined by the cost function $\mathbf{J}_{PD}$. Meanwhile, it always requires a response to a non-zero reference or a step change in actual operation. Therefore, it is necessary to introduce a reference input $\mathbf{x}_{ref}$ to the existing control structure to command the state variables to the desired non-zero values.

In the steady state (SS) when the reference states $\mathbf{x}_{ref}$ are attained, equation (10) can be written as:

$$\mathbf{x}_{ss} = \mathbf{x}_{ref} = \mathbf{\Phi}\mathbf{x}_{ref} + \mathbf{\Gamma}_i \mathbf{u}_{ref,i} \quad (16)$$

Equation (16) can be solved for:

$$\mathbf{u}_{ref,i} = \mathbf{\Gamma}_i^{-1}(\mathbf{I} - \mathbf{\Phi})\mathbf{x}_{ref} = \mathbf{N}_{u,i}\mathbf{x}_{ref} \quad (17)$$

Note that the effect from the state feedback channel should be subtracted from the steady state control input $\mathbf{u}_{ref,i}$. Thus the feedforward gain $\mathbf{N}_{ff,i}$ for introducing the reference input can be designed as:

$$\mathbf{N}_{ff,i} = \mathbf{N}_{u,i} + \mathbf{K}_i$$

Then the feedforward control law can be given as:

$$\mathbf{u}_{ff,i} = \mathbf{N}_{ff,i}\mathbf{x}_{ref}$$

which is shown in Fig.5. Note that $\mathbf{N}_{ff,i}$ is also the *p*-periodic constant gain matrix.

E. Feedforward Rejection of Measurable Disturbances

In order to implement disturbance rejection, a model including disturbance effects is considered and discretized as:

$$\begin{aligned}\mathbf{x}(k+1) &= \mathbf{\Phi}\mathbf{x}(k) + \mathbf{\Gamma}_i \mathbf{u}(k) + \mathbf{\Gamma}_{d,i}\mathbf{v}_{dq}(k) \\ &= \mathbf{\Phi}\mathbf{x}(k) + \mathbf{\Gamma}_i(\mathbf{u}(k) + \mathbf{\Gamma}_i^{-1}\mathbf{\Gamma}_{d,i}\mathbf{v}_{dq}(k))\end{aligned} \quad (18)$$

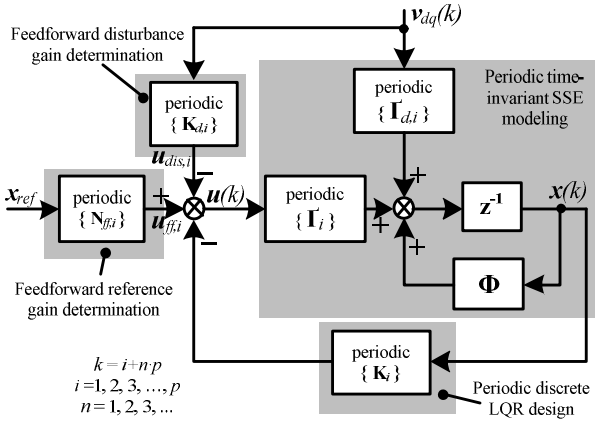

Fig. 5. PDLQR design for Hexverter.

The simplest case is when the disturbances enter the input channel and a feedforward gain $\mathbf{K}_{d,i} = \mathbf{\Gamma}_i^{-1}\mathbf{\Gamma}_{d,i}$ is determined for the measurable disturbances. By applying the control component $\mathbf{u}_{dis,i} = -\mathbf{K}_{d,i}\mathbf{v}_{dq}(k)$ to the control inputs $\mathbf{u}(k)$, disturbances in the *k*-th discretization period can be cancelled by:

$$\mathbf{x}(k+1) = \mathbf{\Phi}\mathbf{x}(k) + \mathbf{\Gamma}_i(-\mathbf{K}_{d,i}\mathbf{v}_{dq}(k)) + \mathbf{\Gamma}_{d,i}\mathbf{v}_{dq}(k) = \mathbf{\Phi}\mathbf{x}(k)$$

which is now independent of $\mathbf{v}_{dq}(k)$.

As a conclusion, the proposed multivariable control structure is presented in Fig.5. The control configuration implements optimal control for the Hexverter's five independent current variables, reference input tracking and measurable disturbance rejection. Note that all of the *p*-periodic matrices can be calculated and stored beforehand. By periodically applying the corresponding control gain matrix $\mathbf{K}_i$ and the feedforward gain matrices $\mathbf{N}_{ff,i}$ and $\mathbf{K}_{d,i}$ to update the control structure, the modeled Hexverter can be controlled. The presented state feedback control can be implemented by a lookup-table (LUT), which is of great advantage for real-time requirements.

V. SIMULATION

A simulation model of the Hexverter based on SSEs is established and it contains the proposed multivariable control design. The Hexverter is required to achieve direct energy conversion from System1-UVW to System2-RST, and a digital controller is implemented to control both d-axis active currents and to suppress the two q-axis reactive and circulating currents. Therefore, the whole system transfers the active power from one grid to another while guaranteeing a unity power factor for both-side grids. The simulation parameters are summarized in Table II. Some explanations should address the two periods in the table, the discretization period T_d and the simulation time T_s. T_d depends on the

TABLE II
CIRCUIT PARAMETERS AND SIMULATION SETTING

Hexverter	Branch resistance	R	0.1 Ω
	Branch inductance	L	2.2 mH
	Number of SMs per branch	N	10
	Nominal SM voltage	U_{SM}	100 V
System1-UVW	Voltage magnitude	U_1	220 V
	Voltage frequency	f_1	50 Hz
	Initial phase angle	θ_1	0
	Resistance	R_1	1 Ω
	Inductance	L_1	10 mH
System2-RST	Voltage magnitude	U_2	110 V
	Voltage frequency	f_2	30 Hz
	Initial phase angle	θ_2	π/3
	Resistance	R_2	0.8 Ω
	Inductance	L_2	15 mH
Difference voltage between N and O		u_N	0 V
Number of samples per hyper-period		p	500
Discretization period for LTI subsystems		T_d	0.2 ms
Simulation time step		T_s	0.02 ms
Simulation steps		N_s	5000
Error weighted matrix		**Q**	diag(22, 44, 11, 22, 50)
Control weighted matrix		**R**	diag(4, 40, 8, 80, 20)

hyper-frequency T_h of the two AC systems and the selected number of samples p per hyper-period. By choosing a comparatively larger p, a better approximation can be achieved when transferring the original continuous LTV system into p-periodic discrete LTI system. Meanwhile, more periodic gains must be accordingly calculated, which requires a large-scale LUT. In the simulation, one discretization interval T_d is equally subdivided into N_s simulation steps and each step amounts T_s ($T_s = T_d / N_s$). According to the sampling principals, a better control performance can be achieved by increasing N_s or by decreasing T_s. The introduced T_s allows the high-speed ADC channels to be fully utilized with the volume of the LUTs reduced and the updating times of the controller parameters limited. The weighting matrices **Q** and **R** are chosen as constant diagonal matrices and they guarantee good overall performance.

The performance of the proposed control design is analyzed in terms of both steady state operation and dynamic step response. In Fig.6(a), the d-axis current from System1 is set to be 20A and accordingly the d-axis current at System2 can be calculated as 31.24A based on the conservation of the power relationship. The input reference $\mathbf{x}_{ref}$ is then set to $[20 \quad 0 \quad 31.24 \quad 0 \quad 0]^T$, which realizes active power transmission from System1 to System2 and high power factors at the both-side voltage sources. The both-side terminal currents are controlled to closely track the reference

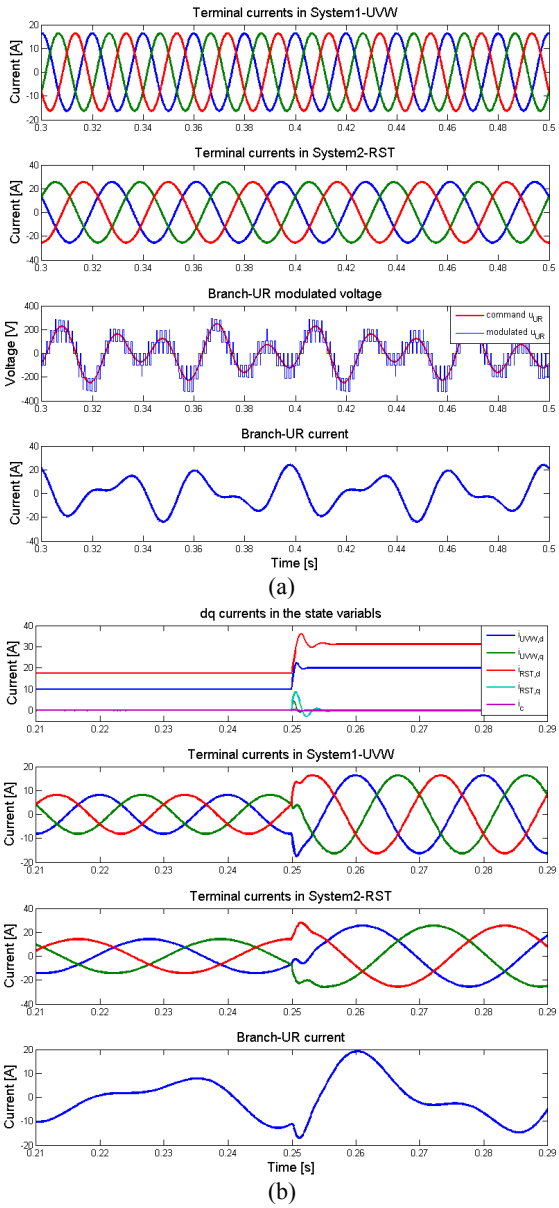

Fig. 6. Simulation results in steady operation and step response to a reference change.

input with a good sinusoidal shape. It can also be seen that the Branch-UR contains two frequency components from the both-side grids and has a hyper-period of 0.1s. To test the dynamic response for a step reference, the reference input is set to be $\mathbf{x}_{ref(t<0.25)} = [10 \quad 0 \quad 17.45 \quad 0 \quad 0]^T$ and then changed at 0.25s to $\mathbf{x}_{ref(t\geq 0.25)} = [20 \quad 0 \quad 31.24 \quad 0 \quad 0]^T$. In Fig.6(b) the PDLQR controller shows a quick response to the reference input change and a uniform convergence rate for all five current variables. The PDLQR controller inherently deals with the complicated coupling among the five current variables and achieves an overall good compromise between state variables tracking and control effort saving, as defined in the chosen cost function.

VI. CONCLUSIONS

This paper presents a direct three-phase AC/AC multilevel converter-Hexverter (DDFB-MMCC) and its state-space modeling in the *abc* and *dq* frames. An equivalent method is applied by treating the Hexverter as two independent single-delta structures with respective frequencies. Thus the overlapping double-frequency voltage components can be decomposed into two respective frequencies and the Park transformation is applicable to the derived SSE model under their respective rotating *dq* frames. Based on the state-space representation, a periodic discretization method is proposed to transfer the original LTV system into a periodic discrete LTI system. Therefore, state feedback control can be implemented to regulate the multiple state variables in an optimal way defined by the cost function. By introducing feedforward control, a reference input can be added to the existing control structure and measurable disturbances can also be well rejected. The simulation results show the effectiveness and performance of the proposed multivariable control strategy in dealing with multiple-input and multiple-output Hexverter systems.

APPENDIX

The applied transformation matrices for deriving the *dq* model of the Hexverter are as follows:

$$\mathbf{T}_{2s/3s,x}=\sqrt{\frac{2}{3}}\begin{bmatrix}1 & 0 & 0 & 0 & 0\\ -\frac{1}{2} & \frac{\sqrt{3}}{2} & 0 & 0 & 0\\ 0 & 0 & 1 & 0 & 0\\ 0 & 0 & -\frac{1}{2} & \frac{\sqrt{3}}{2} & 0\\ 0 & 0 & 0 & 0 & 1\end{bmatrix}$$

$$\mathbf{T}_{2s/3s,u}=\sqrt{\frac{2}{3}}\begin{bmatrix}1 & 0 & 0 & 0 & 0 & 0\\ -\frac{1}{2} & \frac{\sqrt{3}}{2} & 0 & 0 & 0 & 0\\ 0 & 0 & 1 & 0 & 0 & 0\\ 0 & 0 & -\frac{1}{2} & \frac{\sqrt{3}}{2} & 0 & 0\\ 0 & 0 & 0 & 0 & 1 & 0\\ 0 & 0 & 0 & 0 & 0 & 1\end{bmatrix}$$

$$\mathbf{T}_{2s/3s,v}=\sqrt{\frac{2}{3}}\begin{bmatrix}1 & 0 & \frac{1}{\sqrt{2}} & 0 & 0 & 0\\ -\frac{1}{2} & \frac{\sqrt{3}}{2} & \frac{1}{\sqrt{2}} & 0 & 0 & 0\\ -\frac{1}{2} & -\frac{\sqrt{3}}{2} & \frac{1}{\sqrt{2}} & 0 & 0 & 0\\ 0 & 0 & 0 & 1 & 0 & \frac{1}{\sqrt{2}}\\ 0 & 0 & 0 & -\frac{1}{2} & \frac{\sqrt{3}}{2} & \frac{1}{\sqrt{2}}\\ 0 & 0 & 0 & -\frac{1}{2} & -\frac{\sqrt{3}}{2} & \frac{1}{\sqrt{2}}\end{bmatrix}$$

$$\mathbf{T}_{2r/2s,x}=\begin{bmatrix}\cos\varphi_1 & -\sin\varphi_1 & 0 & 0 & 0\\ \sin\varphi_1 & \cos\varphi_1 & 0 & 0 & 0\\ 0 & 0 & \cos\varphi_2 & -\sin\varphi_2 & 0\\ 0 & 0 & \sin\varphi_2 & \cos\varphi_2 & 0\\ 0 & 0 & 0 & 0 & 1\end{bmatrix}$$

$$\mathbf{T}_{2r/2s,u}=\begin{bmatrix}\cos\varphi_1 & -\sin\varphi_1 & 0 & 0 & 0 & 0\\ \sin\varphi_1 & \cos\varphi_1 & 0 & 0 & 0 & 0\\ 0 & 0 & \cos\varphi_2 & -\sin\varphi_2 & 0 & 0\\ 0 & 0 & \sin\varphi_2 & \cos\varphi_2 & 0 & 0\\ 0 & 0 & 0 & 0 & 1 & 0\\ 0 & 0 & 0 & 0 & 0 & 1\end{bmatrix}$$

$$\mathbf{T}_{2r/2s,v}=\begin{bmatrix}\cos\varphi_1 & -\sin\varphi_1 & 0 & 0 & 0 & 0\\ \sin\varphi_1 & \cos\varphi_1 & 0 & 0 & 0 & 0\\ 0 & 0 & 1 & 0 & 0 & 0\\ 0 & 0 & 0 & \cos\varphi_2 & -\sin\varphi_2 & 0\\ 0 & 0 & 0 & \sin\varphi_2 & \cos\varphi_2 & 0\\ 0 & 0 & 0 & 0 & 0 & 1\end{bmatrix}$$

ACKNOWLEDGMENT

This work was partly supported by the National High Technology Research and Development Program of China (863 Program) under Grant No. 2011AA050403.

REFERENCES

[1] M. Glinka, "Prototype of multiphase modular-multilevel-converter with 2 MW power rating and 17-level-output -voltage," *Power Electronics Specialists Conference*, Vol. 4, pp. 2572- 2576, 2004.

[2] H. Akagi, "Classification, Terminology, and Application of the Modular Multilevel Cascade Converter (MMCC)," *IEEE Trans. Power Electron.*, Vol. 26, No. 11, pp. 3119-3130, 2011.

[3] Y. Wan, S. Liu, and J. Jiang, "Generalized analytical methods and current-energy control design for Modular Multilevel Cascade Converter (MMCC)," *IET Power Electronics*. (Accepted)

[4] A. Lesnicar and R. Marquardt, "An innovative modular multilevel converter topology suitable for a wide power range," *Proc. Power Tech Conference*, Vol. 3, pp. 23-26, 2003.

[5] Siemens - HVDC PLUS-http://www.energy.siemens.com/nl/pool/hq/power-transmission/HVDC/HVDC_Plus_Basics_and_Principle.pdf, March 3rd 2013.

[6] L. Baruschka and A. Mertens, "A new 3-phase direct modular multilevel converter," *Power Electronics and Applications, Proceedings of the 2011-14th European Conference on* , pp. 1-10, 2011.

[7] L. Baruschka and A. Mertens, "A new 3-phase AC/AC modular multilevel converter with six branches in hexagonal configuration," *IEEE Energy Conversion Congress and Exposition*, pp. 4005-4012, 2011.

[8] A. J. Korn, M. Winkelnkemper, P. Steimer, and J. W. Kolar, "Direct modular multi-level converter for gearless low-speed drives," *in Proceeding of Power Electronics and Applications*, pp. 1-7, 2011.

[9] P. Munch, S. Liu, and M. Dommaschk, "Modeling and current control of modular multilevel converters considering actuator and sensor delays," *IECON*, pp. 1633-1638, 2009.

[10] P. Munch, S. Liu, and G. Ebner, "Multivariable current control of Modular Multilevel Converters with disturbance rejection and harmonics compensation," *IEEE International Conference of Control Applications*, pp. 196-201, 2010.

[11] P. Munch, D. Gorges, M. Izak, and S. Liu, "Integrated

current control, energy control and energy balancing of Modular Multilevel Converters," *IECON*, pp. 150-155, 2010.
[12] M. Hagiwara, H. Akagi, "Control and experiment of pulsewidth-modulated modular multilevel converters," *IEEE Trans. Power Electron.,* Vol. 24, No. 7, pp. 1737-1746, Jul. 2009.
[13] M. Glinka, R. Marquardt, "A new AC/AC-multilevel converter family applied to a single-phase converter," *International Conference on Power Electronics and Drive Systems*, pp. 16- 23, 2003.
[14] M. Saeedifard and R. Iravani, "Dynamic performance of a modular multilevel back-to-back HVDC system," *IEEE Trans. Power Del.*, Vol. 25, No. 4, pp. 2903-2912, Oct. 2010.
[15] C. Oates, "A methodology for developing 'Chainlink' converters," *European Conference on Power Electronics and Applications*, pp.1-10, 2009.
[16] M. Hagiwara, R. Maeda, and H. Akagi, "Negative-sequence reactive - power control by a PWM STATCOM Based on a Modular Multilevel Cascade Converter (MMCC-SDBC)," *IEEE Trans. Ind. Appl*., Vol. 48, No. 2, pp.720-729, Mar./Apr. 2012.
[17] P. Münch, "Konzeption und entwurf integrierter regelungen für modulare multilevel umrichter," Logos Verlag Berlin GmbH, 2011.
[18] S. Bittanti, P. Colaneri, *Periodic Systems: Filtering and Control. Communication and Control Engineering*, Springer, London, 2009.
[19] G. F. Frankin, J. D. Powell, and A. Emami-Naeini, *Feedback Control of Dynamic Systems*, V. O'Brien, Ed Person Prentice Hall, chap. 8, 2006.
[20] G. F. Franklin, J. D. Powell, and M. L. Workman, *Digital Control of Dynamic Systems*, Addison-Wesley Publishing Company, chap. 8, 1998.
[21] K. J. Astroem, B. Wittenmark, *Computer-controlled Systems–Theory and Design*, second edition. Prentice Hall, chap. 11, 1990.
[22] P. P. Albertos and A. Sala, *Multivariable Control Systems: An Engineering Approach*, London: Springer, chap. 7, 2004.

Yun Wan was born in Nanchang, China, in 1985. He received his B.S. and M.S. in Electrical Engineering from Shanghai Jiao Tong University, Shanghai, China, in 2007 and 2009, respectively. He is currently working toward his Ph.D. from the Key Laboratory of Control of Power Transmission and Conversion, Shanghai Jiao Tong University, Shanghai, China, in cooperation with the Institute of Control Systems, University Kaiserslautern, Kaiserslautern, Germany. His current research interests include multilevel VSC technologies and FPGA for power electronics applications.

Steven Liu received his Dipl.-Ing. and Dr.-Ing. degrees from Technische Universität Berlin, Berlin, Germany, in 1986 and 1992, respectively. He worked with AEG, Germany, Daimler-Benz Research, Germany, and Harz University of Applied Studies and Research, Wernigerode, Germany, before he joined the University of Kaiserslautern, Kaiserslautern, Germany, as a Full Professor, in 2004. His current research interests include control of mechatronic and power systems, robotics, optimization of embedded control, and model-based fault diagnosis.

Jianguo Jiang was born in China, in 1956. He received his Ph.D. in Electrical Engineering from the China University of Mining and Technology, Xuzhou, China, in 1988. He is currently a Professor of Electrical Engineering at Shanghai Jiao Tong University, Shanghai, China. His current research interests include power drives, smart grids, and new energy technology.